JOURNAL OF GEOPHYSICAL RESEARCH, VOL. 103, NO. A4, PAGES 6585-6593, APRIL 1, 1998

The relationship between large-scale solar magnetic field evolution and coronal mass ejections

J. G. Luhmann
Space Sciences Laboratory, University of California, Berkeley

J. T. Gosling
Los Alamos National Laboratory, Los Alamos, New Mexico

J. T. Hoeksema and X. Zhao
Center for Space Science and Astrophysics, Stanford University, Palo Alto, California

Abstract. The idea that coronal mass ejections (CMEs) originate from the evolution of the large-scale solar field and in particular arise from regions of freshly opening coronal flux is reexamined using a new approach. Potential field models constructed from Wilcox Solar Observatory magnetograms are applied to study both the rate of "opening" of coronal fields with time and the locations of observed CMEs compared to the inferred newly open field regions on the Sun. Case studies are drawn from SMM coronagraph data, Yohkoh soft X ray images, and counterstreaming electron events observed on the ICE spacecraft. The results suggest that the large-scale field evolution paradigm of CMEs deserves further attention and has potential for applications to "space weather" forecasting.

1. Introduction

A primary goal of both solar/heliospheric physics and space weather forecasting is to understand what gives rise to coronal mass ejections (CMEs). From a solar physics perspective, CMEs represent a type of solar cycle dependent activity with as yet unclear relationships to other events such as flares or erupting filaments [e.g., *Gosling et al.*, 1992; *Webb and Howard*, 1994; *Bothmer and Schwenn*, 1994; *Cliver et al.*, 1994]. In particular, the roles of solar flux emergence [e.g., *Feynman and Martin*, 1995], surface and subsurface velocity shears [e.g., *Linker and Mikic'*, 1995], and magnetic reconnection [e.g., *Gosling et al.*, 1995] in the overall CME process continue to be debated. While it has been considered for some time that CMEs are a part of large-scale coronal magnetic field evolution [e.g., *Sime*, 1989; *Low*, 1996; *Harrison et al.*, 1990; *McComas*, 1994], this connection has not been explored in much detail. In contrast, on the space weather side it has been convincingly demonstrated that large geomagnetic storms are the response of the magnetosphere to interplanetary disturbances produced by fast CMEs [e.g., *Gosling et al.*, 1990]. It is moreover understood that the geomagnetic "effectiveness" of a particular CME is determined largely by the size of its associated VB_s (where V is the plasma speed and B_s is the magnitude of the southward interplanetary magnetic field component). Enhanced magnetospheric responses usually result if there is a preceding interplanetary shock or if the disturbance dynamic pressure is particularly high. Thus the interplanetary aspects of CMEs important to space weather are relatively well understood [e.g., *Webb*, 1995]. At the same time, we lack the ability to determine whether a potentially geoeffective CME has left the Sun on an Earth-bound trajectory, a problem that relates to the solar origin issues. This is probably the major factor in the less than exemplary geomagnetic storm forecasting record [e.g., *Joselyn*, 1995].

Here we describe tests of the viewpoint that large-scale coronal magnetic field evolution originating from changes in the Sun's internal field is the cause of CMEs. CMEs are collectively viewed as the manifestations of initially "closed" field regions on the Sun becoming open to interplanetary space in response to changes in the solar field. Our picture thus excludes changes in coronal field structure that are purely coronal in origin. To test this hypothesis, we use model coronal fields derived from ground-based magnetograms to locate the newly opening regions, together with several types of observational signatures of CME occurrence: coronagraph images, soft X ray images, and counterstreaming suprathermal electrons observed in the solar wind. We find encouraging support for the large-scale field evolution picture and suggest how our approach might be useful for both further studies of CMEs and for space weather prediction.

2. Solar and Interplanetary Magnetic Flux Cycles

The magnetic flux through the visible photosphere is routinely measured at ground-based observatories. Figures 1a and 1b together illustrate the well-known tracking of total photospheric flux and sunspot number [e.g., *Schrijver and Harvey*, 1994]. While it is not so straightforward to make corresponding "global" measurements of the associated interplanetary flux since spacecraft make only single point in situ measurements [e.g., *McComas et al.*, 1992], one can infer the interplanetary flux cycle using extrapolations of potential field-source surface models of the coronal magnetic field if current sheet corrections are included [e.g., *Hoeksema*, 1995; *Zhao and Hoeksema*, 1996; *Wang*, 1995].

Most potential field source surface models are constructed from synoptic (27-day) maps of the photospheric field and impose a spherical outer boundary or "source surface" at R_{ss}=1.6-2.5 R_s (R_s

Paper number 97JA03727.
0148-0227/98/97JA-03727$09.00

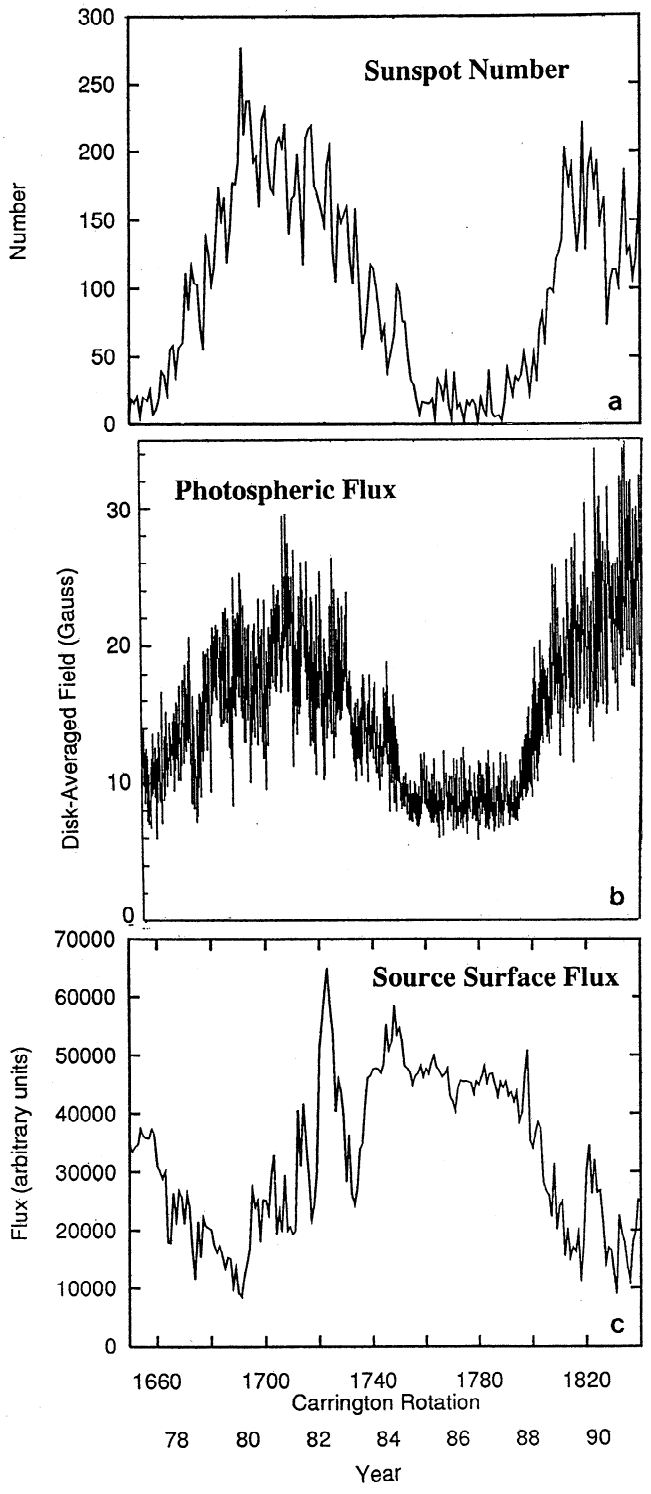

Figure 1. (a) Monthly sunspot number available from the National Solar Observatory home page (http://www.sunspot.noao.edu). (b) Disk-integrated daily photospheric flux from the above reference, also showing the rms deviation. (c) Carrington rotation (27-day) values of the full source surface flux, computed from the WSO potential field models.

is the solar radius) where the field becomes radial. This outer boundary condition serves as a first approximation to the effect of the accelerating solar wind on the coronal field structure, although the current sheet corrections mentioned above produce a better approximation in the outer regions. Apparent departures from potential field behavior are also found at the photosphere, where the magnetic field appears to be more nearly radial than potential [e.g., *Wang and Sheeley*, 1992; *Zhao et al.*, 1997], and around active regions, where the field is very dynamic [e.g. *Altschuler et al.*, 1977]. To address the former, many potential field source surface models now apply a radial field condition at the photospheric inner boundary as well as at the source surface. The departure from potentiality associated with dynamics is more difficult to correct, but at least before and after transients, potential field models appear to be a reasonably good approximation to the large scale coronal field. They provide accurate descriptions of the interplanetary field polarity based on the source surface field [e.g., *Hoeksema*, 1995], compare favorably with eclipse and coronagraph observations of the corona [e.g., *Altschuler et al.*, 1977], and perhaps most important here, reproduce the geometry of coronal hole boundaries [e.g., *Levine*, 1982] when the inferred open field lines are traced to the solar surface.

The present study uses potential field source surface models derived from synoptic photospheric field maps from the Wilcox Solar Observatory (WSO) to study changes in the large-scale coronal field. The synoptic maps that provide the inner boundary conditions for the coronal field models are constructed from daily full-disk magnetograms. The models are corrected for "monopolar" contributions that arise from the synoptic map construction method. They are available as an archived set of spherical harmonic coefficients for each Carrington Rotation since CR 1642 (June 1976). They thus provide a means of analyzing changes in the coronal field with time for solar cycle intervals. A source surface radius of 2.5 R_s is used because of its success in reproducing the observed interplanetary field polarity.

Changes in the magnetic flux through the source surface corresponding to those observed over the same time interval in the photosphere (Figure 1b) are shown in Figure 1c. The total source surface flux is nearly anticorrelated with the sunspot number, in contrast to the photospheric flux behavior, but consistent with estimates of the interplanetary flux cycle [e.g., *McComas et al.*, 1992; *Wang*, 1995]. This result is easy to understand because most of the strong flux erupting from the photosphere as the Sun approaches solar maximum occurs in small-scale regions, including sunspots. These regions generally produce high-order harmonic contributions to the solar field that do not extend far into the corona. Indeed, comparison of the time history of the source surface flux with the contributions of various harmonics to the WSO potential field models in Figure 2, shows that the source surface flux history is almost a replica of the dipole contribution history. Only for a few intervals during high solar activity periods do the first few higher-order (quadrupolar and octupolar) terms make contributions comparable to the dipole (also see *Obridko and Shelting* [1992]).

Increases in the flux out of the source surface caused by changes in the photospheric field are of most interest here. If the assumption that CMEs are the primary means by which new solar flux becomes opened to interplanetary space (as in the work of *McComas* [1994, and references therein]) is correct, we should be able to find both statistical and individual event evidence of that relationship in observations. One possible statistical test is to ask whether the average increases in flux out of the source surface, evident in Figure 1c, behave like the long-term CME rate. If we assume that a positive (absolute) flux change between any two Carrington rotations within a year is proportional to the number of CMEs ejected, and neglect flux decreases during the same period (presumably related to regions of the coronal field that are closing

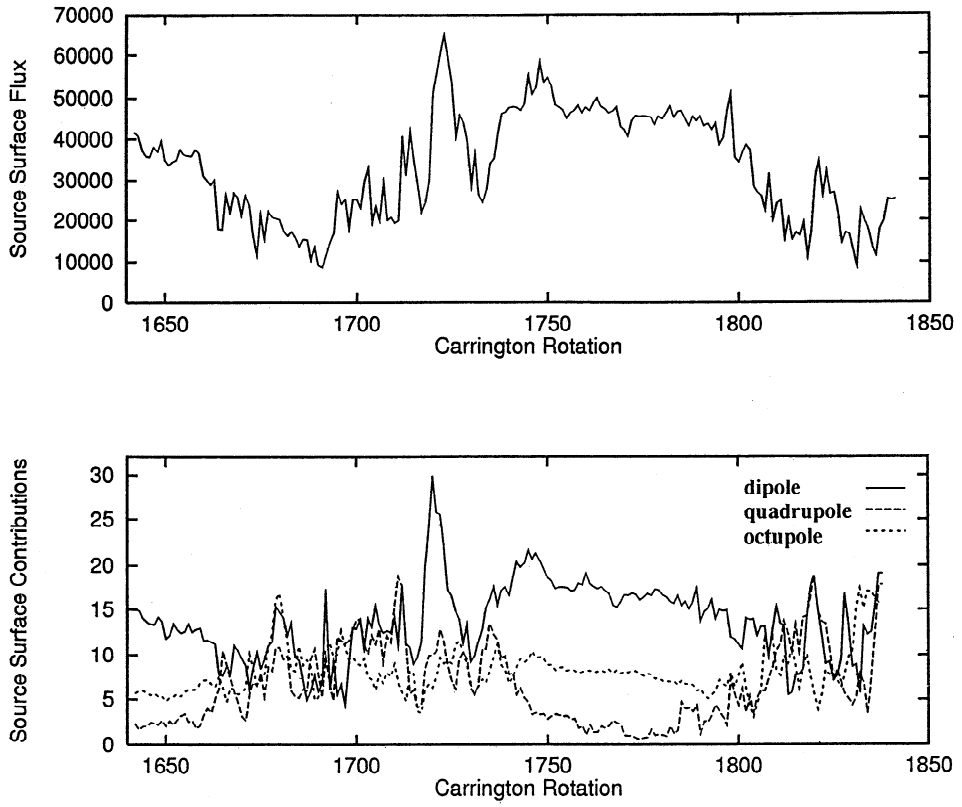

Figure 2. (top) Carrington rotation (27-day) values of the source surface flux compared to the (bottom) contributions of the three lowest order moments to the source surface flux. The total source surface flux history closely resembles the dipole contribution. The normalization procedure of *Hoeksema and Scherrer* [1986] is used in the bottom panel scale.

down), we obtain the annual average rates of flux addition shown in Figure 3. The basic agreement between the temporal behavior of the annual averages of inter-Carrington rotation source surface flux increases, and the CME rates determined from a variety of observations, both support our assumptions regarding CMEs' role in interplanetary flux cycles and provides motivation for case studies.

For case studies of specific CMEs it is necessary to locate the regions of newly open coronal flux. The approach we use here involves tracing field lines in the potential model between the photosphere and the source surface for consecutive potential models. A dense (1° × 1°) latitude-longitude grid is adopted for starting field lines, and the potential field model is restricted to the first nine harmonics to make the repetitious evaluation of the field in the field line tracing computations efficient. We presumed that wherever field lines from the photosphere become newly connected to the source surface between consecutive models, a transient has occurred in the interim where previously closed flux tubes were stretched out into interplanetary space. We assume that these transients represent CMEs and that the times and locations of the new connections mark the times and locations of CMEs. As an illustration of this approach, Figure 4 shows only those field lines from the tracing procedure that were closed on CR (Carrington rotation) 1747 but open on CR 1748. (All other field lines either remained closed or open.) The field lines shown are thus regarded as an effective "image" of all of the CMEs that occurred between these two Carrington rotations. Below we describe some sample observational tests using specific examples from several types of CME data.

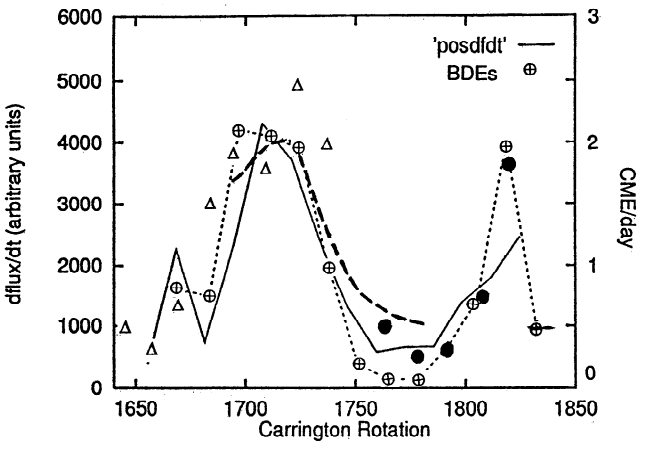

Figure 3. Comparison of the annual rate of addition of new flux to the source surface (e.g., the annual average of the positive derivatives of the data plotted in Figure 1c) with the (normalized) rate of CME occurrence from several sources. The symbols connected by the dotted line show the time history of counterstreaming solar wind electron events (BDEs), considered an interplanetary signature of CMEs, from *Gosling et al.* [1992]. The other symbols and the dashed line are from a survey of coronagraph records by *Webb and Howard* [1994]. The scale on the right pertains to the latter data.

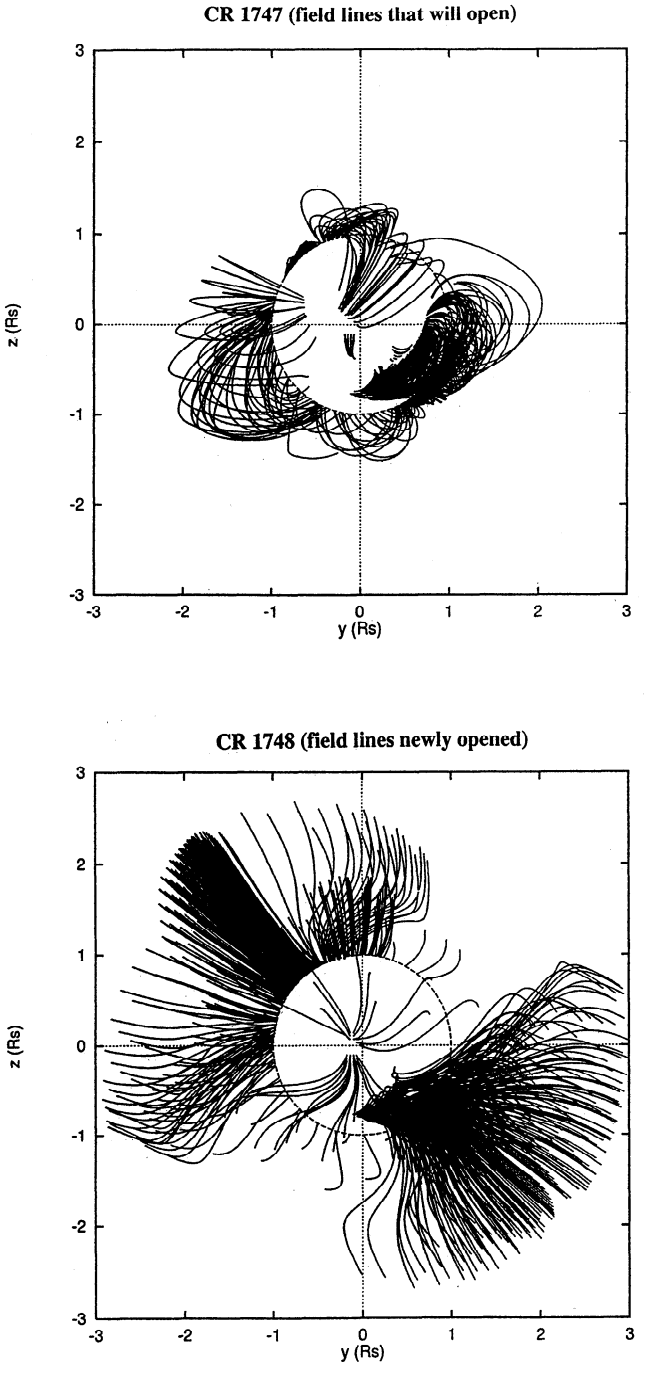

Figure 4. Projection of three-dimensional coronal potential model field lines, described in the text, that were closed on CR 1747 and open on CR 1748. It is suggested that these represent the sites of CMEs that occurred between these two Carrington Rotations. (CR 1747 covers March 31 to April 26, 1984; CR 1748 covers April 27 to May 23, 1984.)

3. Comparisons With Observational Signatures of CMEs

Both remote sensing and in situ data have been used to detect CMEs, whose ubiquity was first appreciated during the operation of the Skylab coronagraph [e.g., *Gosling et al.*, 1974]. CMEs were later monitored and catalogued for a significant part of a solar cycle with the Solar Maximum Mission coronagraph [e.g., *Burkepile and St. Cyr*, 1993]. In situ interplanetary measurements of counterstreaming solar wind electrons were found to be a reliable signature of the CME extensions into interplanetary space [e.g., *Gosling et al.*, 1987], and transients in coronal plumes and arcade structures observed on Yohkoh in soft X rays were sometimes found to precede such signatures [see *Winterhalter et al.*, 1996]. Because CMEs as observed in coronagraph images erupt in minutes to hours (although the regions from which they arise may remain a source of CMEs for weeks), the synoptic maps might not capture an individual event signature. In particular, these maps are weighted by central meridian daily magnetogram data that does not necessarily include the site of a CME-related change on that particular day. However, since we assume a CME is associated with a change in the large-scale solar field, evidence could persist for a time provided that subsequent alterations in the fields contributing to the synoptic map do not obliterate those of interest. Such conditions are most likely to hold during minimum solar activity periods when the solar field evolves slowly. We thus examined the SMM coronagraph images of solar minimum period CMEs (J. Burkepile and J. Gurman, personal communication, 1995), Yohkoh team reports of CME-related coronal structures, and previously published lists of counterstreaming electron events observed on ICE (previously ISEE 3) from solar minimum periods. Below we show an example from each data set that appears to provide further support for our adopted CME paradigm.

3.1. SMM Coronagraph Example

Images of a solar minimum CME from the SMM coronagraph catalogue compiled by *Burkepile and St. Cyr* [1993] are reproduced in Figure 5a. This event occurred on October 15, 1986, during CR 1781. The images show both the CME and a coronal streamer deflected by the passage of the CME. Figure 5b shows the subset of field lines from the potential field models that were closed on the CR pictured but open on the following CR. The CME at the top right is clearly seen in the inferred freshly opening fields for CR_s 1780 and 1781. (October 15 falls near the boundary between these two Carrington rotations.) Field lines are also inferred to open in the region of the helmet streamer structure on the east (left) limb. The SMM coronagraph catalog in fact notes that a "streamer expands slowly" on October 16-17 at this location. This second event, and the freshly opening fields indicated elsewhere in Figure 5b, seem consistent with the idea [e.g., *Crooker*, 1993] that the helmet streamer belt contains a dynamic mix of opening and closing solar flux tubes that are destined to become embedded in the heliospheric current sheet. The reason why the above CME exploded outward at 719-1241 km/s, while the helmet streamer belt flux tubes expanded at low speeds is an issue beyond the scope of the present study.

3.2. Yohkoh Example

On April 14, 1994, the Yohkoh soft X ray telescope (SXT) recorded what was called a "global restructuring event" [e.g., *Alexander et al.*, 1996]. This event was distinguished by a suddenly brightening coronal plume structure of unusual longitudinal extent in the southern solar hemisphere. Figure 6 displays the SXT images from April 13 and 14 from the Mullard Space Sciences Laboratory on-line archive (http://mssly1.mssl.ucl.ac.uk). The appearance of the bright southern hemisphere structure was followed by both detection of an appropriately located interplanetary CME signature on the Ulysses spacecraft [*Gosling et al.*, 1994] and a geomagnetic storm at the Earth [*McAllister et al.*, 1996].

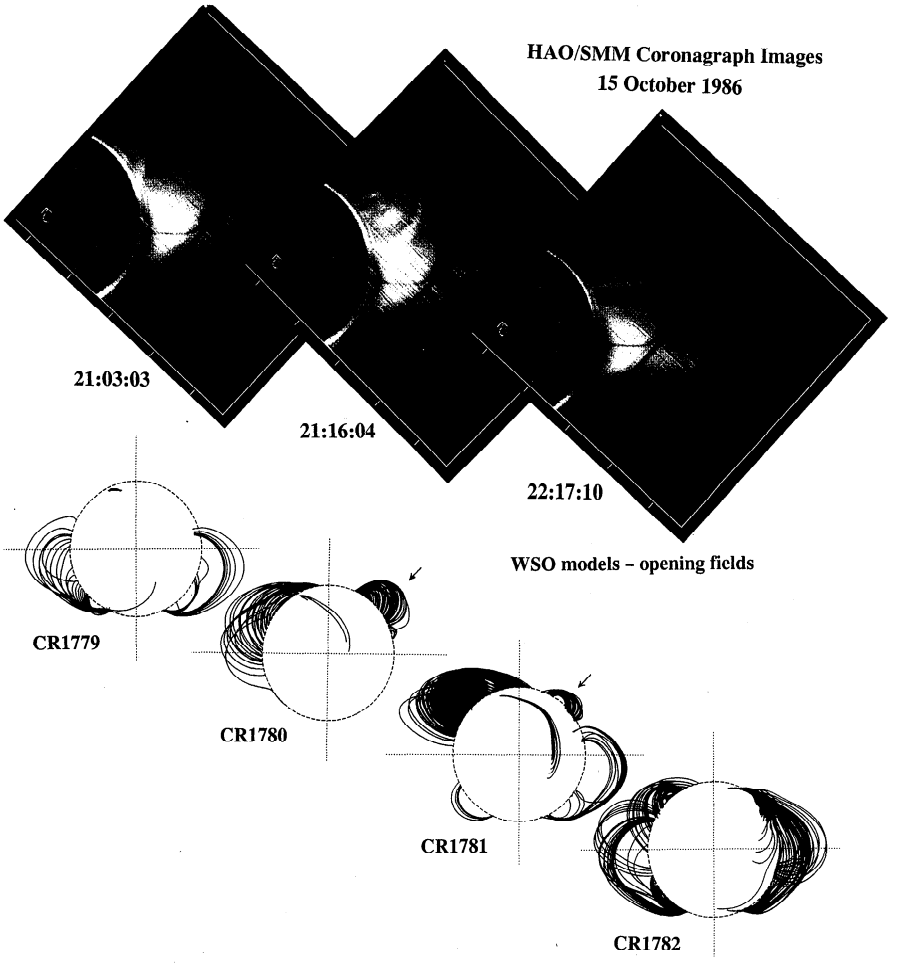

Figure 5. A sequence of images from the (top) SMM coronagraph showing a CME occurring on October 15, 1986 compared to (bottom) "predicted" locations from the newly opening fields occurring during the Carrington Rotation (27-day) periods for CR 1779, CR 1780, CR 1781 and CR 1782. The date of the CME falls almost at the boundary between CR 1780 and CR 1781.

Interestingly, *Alexander et al.* [1996] showed that the potential field model from the Carrington rotations during and after this event did not exhibit substantial differences in large-scale coronal geometry. The field structure included a feature resembling the brightened plume in both, as part of an apparent inclined helmet streamer belt. However, in the present picture of CMEs, coronal field lines can open without an accompanying gross change in the coronal field structure. For example, a change in the dipole moment of a dipole field dominated corona can add new open fields without altering the location of the neutral line on the source surface or the overall appearance of the corona.

In this case where the CME signature is observed far from the limb we can resort to a special method (described by *Zhao et al.* [1997]) to improve the effective temporal resolution of the synoptic models. The daily magnetogram of interest is inserted into the synoptic maps, in essence minimizing the averaging that goes into the visible disk portion of the potential model. A special synoptic map is then constructed with its central Carrington longitude corresponding to the central meridian of the single magnetogram. (Because of foreshortening effects, the magnetogram data are taken only from within 65 deg of the equator and 55 deg of the central meridian passage.) Potential models are derived in the usual way from these tailored synoptic maps to give what are effectively higher time resolution representations of the daily coronal field. The comparison shown in Figure 6, using the special synoptic maps for April 13-14 and April 14-15 to locate the newly opening fields between these pair of days, suggests that the brightened soft X ray structure observed on April 14 and the related interplanetary consequences were associated with newly opening fields. The brightened region in the northwest (top right) in the April 14 Yohkoh SXT image also appears in the field line plot.

3.3. Counterstreaming Electrons as a Diagnostic

The idea that counterstreaming suprathermal interplanetary electrons (bidirectional electrons, BDEs), are the manifestation of "newly opening" solar magnetic flux tubes is not new [e.g., *Gosling et al.*, 1987; *McComas*, 1994]. The beams moving in both directions along the interplanetary field are most naturally explained as the solar heat flux coming from the two ends of a magnetic loop still connected to the Sun as it expands outward. If we assume that BDEs are synonymous with CMEs, we can examine the relationship between BDEs and the large-scale coronal field evolution with the basic approach used above for the SMM coronagraph and Yohkoh SXT CME comparisons. The archived full disk magnetograms from the WSO are available for the interval of time spanning the period 1978-1990 when the ISEE

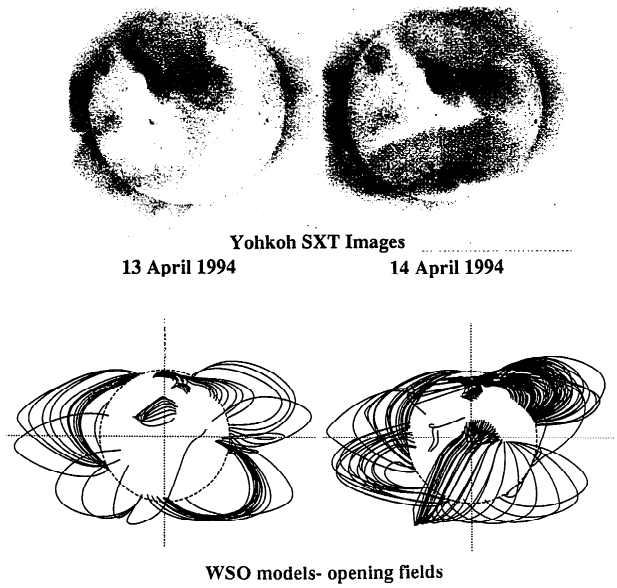

Figure 6. (top) Soft X ray images from Yohkoh SXT for April 13 and 14, 1994, showing "global restructuring" in the corona that preceded an interplanetary detection of a CME and a geomagnetic storm. (bottom) Newly opening field lines between April 13 and 14 and April 14 and 15 computed using special "high-resolution" synoptic maps for the potential field models. These special daily maps are described in the text.

3 spacecraft (ICE after 1983) was monitoring BDE occurrence. In this case, to compare the locations of the newly opened fields in the corona with the times of occurrence of the detected BDEs, we must take account of the delay time associated with the CME transit to 1 AU. For our purposes, we can assume that 4 days or less are required since average CME speeds inferred from BDEs at 1 AU are the same as the average solar wind speed [*Gosling et al.*, 1987].

One of the data sets included in Figure 3 shows how the annual rate of increase of source surface flux contained in the newly opened regions of the photosphere (between Carrington rotations) follows the long-term history of BDEs (normalized for "global" coverage, and for many gaps in tracking in 1984-1987) observed on ICE [from *Gosling et al.*, 1992]. For individual events, however, there are again limitations imposed by the 27-day time resolution of the standard WSO field models, and in this case by the single-point sampling of ICE. To reduce potential confusion introduced by solar fields that evolve on much faster than Carrington rotation time scales, we chose to examine the solar minimum period 1984-1987. Analysis of a particularly unambiguous case, with two isolated CMEs from different regions detected at ICE during CR 1747, is described here.

Figure 7 shows heliolatitude-longitude projections on the Sun of potential model field lines traced from the usual (1° × 1°) grid on the photosphere that were closed (e.g., not connected to the source surface) on CR 1747, but open (e.g. connected to the source surface) on CR 1748 (also see Figure 4). The corresponding dates

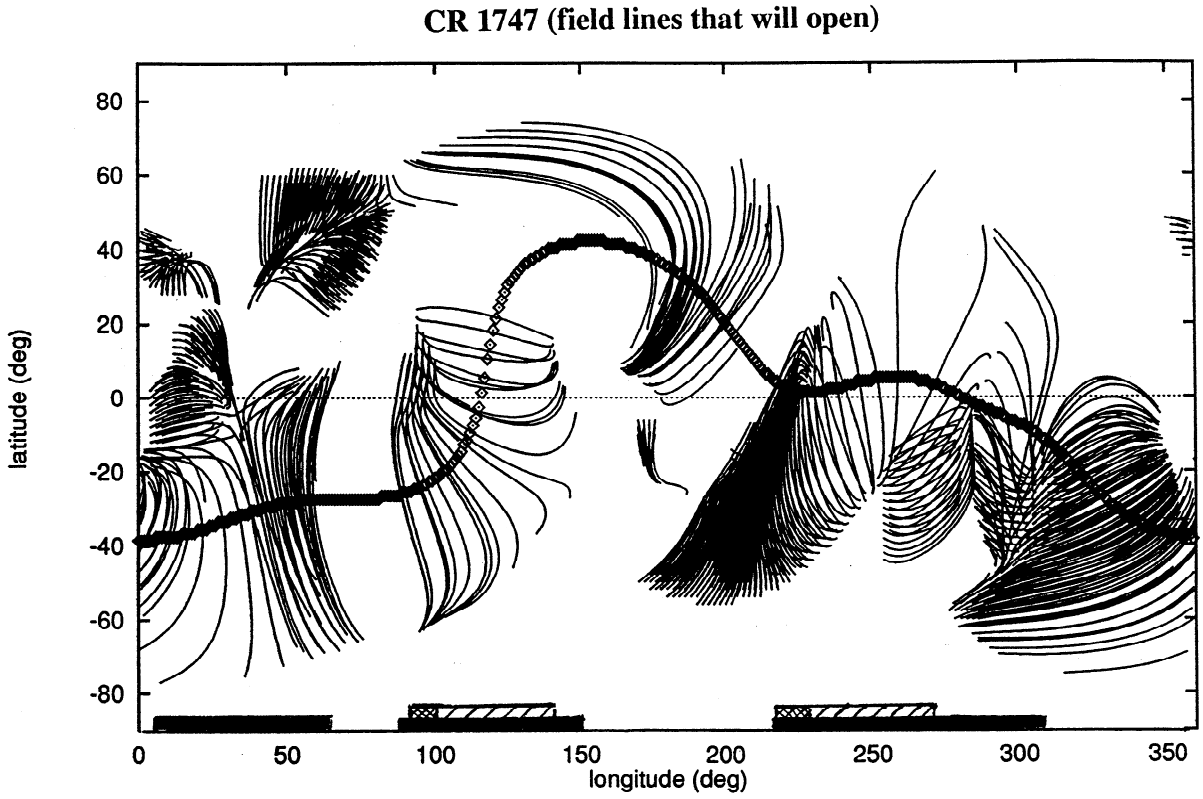

Figure 7. Longitude/latitude projection of potential model field lines originating at locations on the photosphere that became newly connected to the source surface (i.e., open) between CR 1747 and CR 1748. The location of the neutral line on the source surface is shown by the points plotted at every degree of longitude. The shaded bars along the horizontal axis indicate where the still-closed field lines cross the heliographic equator (black bars), and the locations of the central meridian at the times of detected BDEs (cross-hatched bars) with extensions allowing for typical propagation times from the Sun (hatched bars). The intent here is to show that the BDEs occurred within the black bar intervals where flux tube opening was inferred from the models.

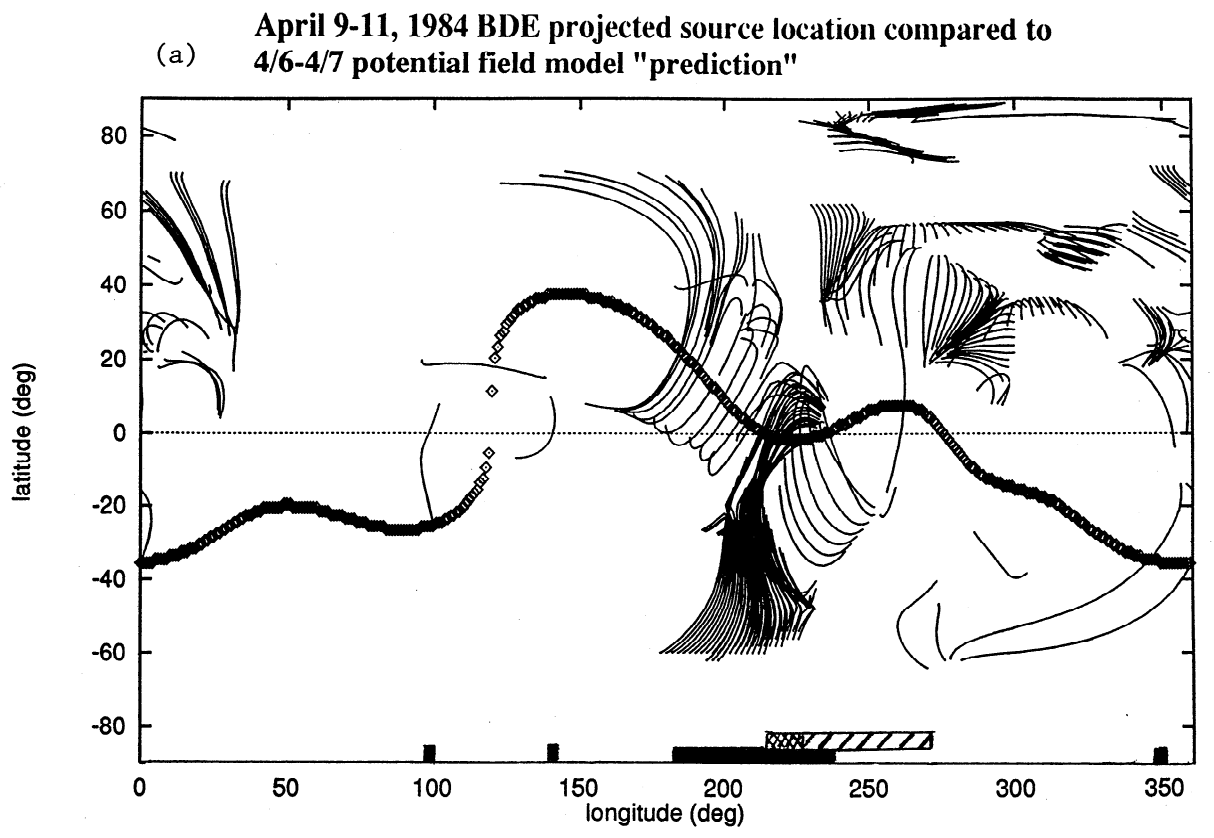

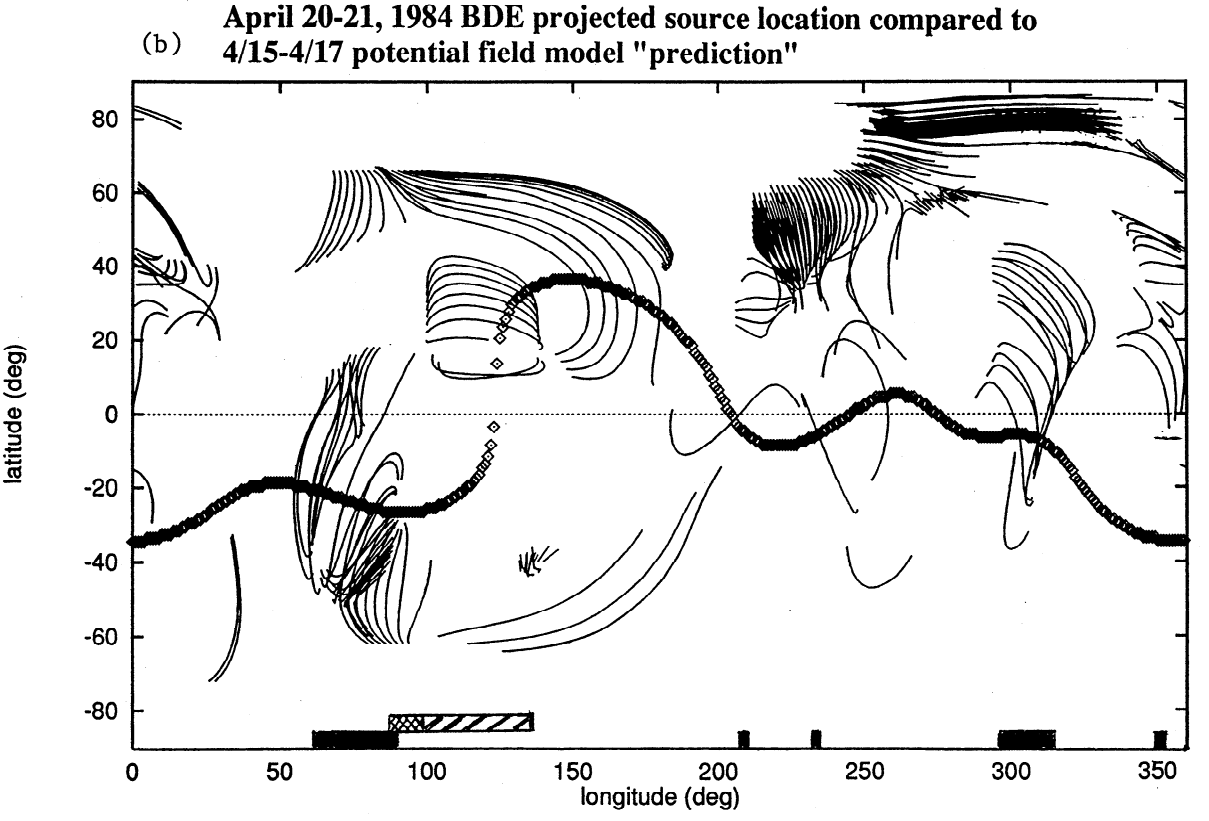

Figure 8. (a) A more accurate approximation to the newly opening flux map around the time of the ISEE-3 April 9-11, 1984 BDE during CR 1747 using daily magnetograms. (See text.) (b) Same as Figure 8a but for the BDE on April 20-21, 1984. In this case, data were not available for April 16, so the inferred opening fields occurred between April 15 and 17.

(equivalent to Carrington longitudes) of BDEs seen at ICE are indicated by the bar chart appended to the longitude axis. The central meridian locations on the actual dates on which the BDEs occurred are indicated by the cross-hatched bars, with the adjacent hatched bars extending up to 4 days earlier take into account the spread of possible transit times. The black bars mark intervals where the preevent closed field lines crossed the solar equator, presumably producing low-heliolatitude BDEs as they opened into interplanetary space. Note that during this period of low solar activity, the black bar intervals coincide with equatorial crossings of the helmet streamer belt, again consistent with previous studies that found an association of CME occurrence with that feature [e.g., *Hundhausen*, 1993; *Crooker et al.*, 1993]. The two ICE events detected during CR 1747 are located within the expected (black bar) regions. Of the other BDEs observed on ICE in the period 1984-1987, over half occurred within the range of interplanetary propagation times for intervals of inferred opening fields. The disagreements may relate to the inherent low time resolution of the synoptic charts used to derive the potential field models, the problem noted above.

In Figure 8 we show an attempt to identify the specific CME/BDE sites using potential models from the special synoptic charts described above. In this case the consecutive dates April 6-7, 1984 (Figure 8a), and April 15-17, 1984 (Figure 8b), were chosen to correspond to the individual CME times. The newly open equatorial field regions shown by the black bars in Figure 8 for these more restricted time intervals are encouragingly consistent with the different locations apparently giving rise to the two BDEs. Unfortunately, we cannot apply this special procedure to most of the BDEs in our data set because unfavorable observing conditions from the ground often interrupt the WSO daily recording of magnetograms. Of course, this limitation would not occur with a space-based magnetograph and/or a global ground-based network.

4. Concluding Remarks

The simple picture of CMEs as evolving large-scale solar field "products," reinforced by this study, provides a potentially powerful framework. For example, if we can think of CME cycles as a reflection of the rate of change of the low-order harmonics of the solar dynamo field, we can begin to envision how their origin can be investigated using helioseismology. We can begin to understand some previous observations such as the failure of CMEs to affect the neutral sheet geometry [*Zhao and Hoeksema*, 1996] (e.g., a dipole strengthening that may lead to new open fields and thereby cause a CME is not necessarily accompanied by a dipole moment reorientation), and the frequent lack of associated photospheric signatures. We can also adopt some new approaches to space weather research and forecasting. The SOHO MDI magnetograph and Wind and ACE instruments will soon provide improved data sets (e.g., higher time resolution (96 min) potential field models and continuous solar wind monitoring) that can be used to locate prospective CME sites. The SOHO data can also be used to examine the attributes (e.g., underlying magnetic structure, magnetic shear, neutral line geometry) that may determine CME speed. The GONG helioseismology project obtains full-disk magnetograms every 20 min from a network of stations distributed around the Earth. These can be used to look for large-scale solar field changes without some of the limitations of spacecraft coverage.

Of course, potential pitfalls exist even beyond the realm of the observational limitations, including those resulting from the assumptions of a constant radius spherical source surface [e.g., see *Schulz*, 1978] and a potential field [e.g., *Altschuler et al.*, 1977] in determining which regions on the Sun are magnetically open or closed. Especially during solar maximum, the fields may change too rapidly for even high time resolution full-disk magnetograms to give an accurate global picture. The reason for the enhanced speeds of a small fraction of CMEs relative to the normal solar wind speeds [e.g., *Hundhausen et al.*, 1994] may in fact be related to departures from a potential field structure, making it difficult to use the above approach to infer which conditions give rise to fast CMEs. This technique also does not take into account the interplanetary evolution of a CME disturbance as it interacts with the structured ambient interplanetary medium, affecting its "geoeffectiveness." Only further investigations will show whether these issues are important barriers to using the paradigm and approach described here.

Acknowledgments. One of the authors (J.G.L.) acknowledges support from the Solar Terrestrial Division of the National Science Foundation ATM Program through grant ATM-9531741. Work (by J.T.G.) at Los Alamos was performed under the auspices of the U.S. Department of Energy with support from an Internal Research and Development Grant, and at Stanford University (by X.P.Z. and J.T.H.) with support from grants NASA NAGW-2502, NASA NAG5-3077, NSF ATM-9400298 and ONR N00014-97-1-0129.

The Yohkoh SXT images used herein were obtained from the Yohkoh Data Archive Center. Yohkoh is a mission of the Japanese Institute for Space and Astronautical Science.

The Editor thanks G. Simnett and E. W. Cliver for their assistance in evaluating this paper.

References

Alexander, D., K.L. Harvey, H.S. Hudson, J.T. Hoeksema, and X. Zhao, The large scale eruptive event of 1994 April 14, in *Solar Wind Eight*, edited by D. Winterhalter *et al.*, *AIP Conf. Proc. 382*, p. 84, Amer. Inst. of Phys., New York, 1996.

Altschuler, M.D., R.H. Levine, M. Stix, and J. Harvey, High resolution mapping of the magnetic field of the solar corona, *Sol. Phys.*, *51*, 345, 1977.

Bothmer, V., and R. Schwenn, Eruptive prominences as sources of magnetic clouds in the solar wind, *Space Sci. Rev.*, *70*, 215, 1994.

Burkepile, J.T., and O.C. St. Cyr, A revised and expanded catalogue of mass ejections observed by the solar maximum mission coronagraph, *NCAR Tech. Note* NCAR/TN-369STR, High Altitude Obs., Natl. Cent. for Atmos. Res., Boulder, Colo., Jan. 1993.

Cliver, E.W., O.C. St. Cyr, R.A. Howard, and P.S. McIntosh, Rotation-averaged rates of coronal mass ejections and dynamics of polar crown filaments, in *Solar Coronal Structures*, *IAU Colloq. 144*, edited by V. Rusin, P. Heinzel, and J.C. Vial, p. 83, VEDA, Bratislava, 1994.

Crooker, N.U., G.L. Siscoe, S. Shodhan, D.F. Webb, J.T. Gosling, and E.J. Smith, Multiple heliospheric current sheets and coronal streamer belt dynamics, *J. Geophys. Res.*, *98*, 9371, 1993.

Feynman, J., and S.F. Martin, The initiation of coronal mass ejections by newly emerging magnetic flux, *J. Geophys. Res.*, *100*, 3355, 1995.

Gosling, J.T., E. Hildner, R.M. MacQueen, R.H. Munro, A.I. Poland, and C.L. Ross, Mass ejections from the Sun: A view from Skylab, *J. Geophys. Res.*, *79*, 4581, 1974.

Gosling, J.T., D.N. Baker, S.J. Bame, W.C. Feldman, and R.D. Zwickl, Bidirectional solar wind electron heat flux events, *J. Geophys. Res.*, *92*, 8519, 1987.

Gosling, J.T., S.J. Bame, D.J. McComas, and J.L. Phillips, Coronal mass ejections and large geomagnetic storms, *Geophys. Res. Lett.*, *17*, 901, 1990.

Gosling, J.T., D.J. McComas, J.L. Phillips, and S.J. Bame, Counterstreaming solar wind halo electron events: Solar cycle variations, *J. Geophys. Res.*, *97*, 6531, 1992.

Gosling, J.T., D.J. McComas, J.L. Phillips, L.A. Weiss, V.J. Pizzo, B.E. Goldstein, and R.J. Forsyth, A new class of forward-reverse shock pairs in the solar wind, *Geophys. Res. Lett.*, *21*, 2271, 1994.

Gosling, J.T., J. Birn and M. Hesse, Three-dimensional magnetic reconnection and the magnetic topology of coronal mass ejection events, *Geophys. Res. Lett.*, *22*, 869, 1995.

Harrison, R.A., E. Hildner, A.J. Hundhausen, D.G. Sime, and G.M. Simnett, The launch of solar coronal mass ejections: Results from the coronal mass ejection onset program, *J. Geophys. Res., 95*, 917, 1990.

Hoeksema, J.T., The large-scale structure of the heliospheric current sheet during the Ulysses epoch, *Space Sci. Rev., 72*, 137, 1995.

Hoeksema, J.T. and P.H. Scherrer, The solar magnetic field 1976 through 2985, *Rep. UAG-94*, U.S. Dep. of Comm., Natl. Oceanic and Atmos. Admin., Boulder, Colo., 1986.

Hoeksema, J.T., J.M. Wilcox, and P.H. Scherrer, The structure of the heliospheric current sheet: 1978-1982, *J. Geophys. Res., 88*, 9910, 1983.

Hundhausen, A.J., The sizes and locations of coronal mass ejections: SMM observations from 1980 and 1984-1989, *J. Geophys. Res., 98*, 13,177, 1993.

Hundhausen, A.J., J.T. Burkepile, and O.C. St. Cyr, Speeds of coronal mass ejections: SMM observations from 1980 and 1984-1989, *J. Geophys. Res., 99*, 6543, 1994.

Joselyn, J.A., Geomagnetic activity forecasting: The state of the art, *Rev. Geophys., 33*, 383, 1995.

Levine, R.H., Open magnetic fields and the solar cycle I, *Solar Phys., 79*, 203, 1982.

Linker, J.A., and Z. Mikic', Disruption of a helmet streamer by photospheric shear, *Astrophys. J., 438*, L45, 1995.

Low, B.C., Solar activity and the corona, *Sol. Phys., 167*, 217, 1996.

McAllister, A.H., M. Dryer, P. McIntosh, H. Singer, and L. Weiss, A large polar crown coronal mass ejection and a "problem" geomagnetic storm: April 14-23, 1994, *J. Geophys. Res., 101*, 13, 497, 1996.

McComas, D.J., Evolution of the interplanetary magnetic field, in *Solar System Plasmas in Space and Time, Geophys. Monogr. Ser.*, vol. 84, edited by J.L. Burch and J.H. Waite Jr., p. 53, A.G.U., Washington, D.C., 1994.

McComas, D.J., J.T. Gosling, and J.L. Phillips, Interplanetary magnetic flux: Measurement and balance, *J. Geophys. Res., 97*, 171, 1992.

Obridko, V.N., and B.D. Shelting, Cyclic variation of the global magnetic field indices, *Sol. Phys., 137*, 167, 1992.

Schrijver, C.J., and K.L. Harvey, The photospheric magnetic flux budget, *Sol. Phys., 150*, 1, 1994.

Schulz, M., E.N. Frazier, and D.J. Boucher, Coronal magnetic-field model with non-spherical source surface, *Sol. Phys., 60*, 83, 1978.

Sime, D.G., Coronal mass ejection rate and the evolution of the large-scale K-coronal density distribution, *J. Geophys. Res., 94*, 151, 1989.

Wang, Y-M., Latitude and solar-cycle dependence of radial IMF intensity, *Space Sci. Rev., 72*, 194, 1995.

Wang, Y-M., and N.R. Sheeley, On potential field models of the solar corona, *Astrophys. J., 292*, 210, 1992.

Webb, D.F., Coronal mass ejections: The key to major interplanetary and geomagnetic disturbances, *U.S. Nat. Rep. Int. Union Geod. Geophys. 1991-1994, Rev. Geophys., 33*, 577, 1995.

Webb, D.F., and R.A. Howard, The solar cycle variation of coronal mass ejections and solar wind mass flux, *J. Geophys. Res., 99*, 4201, 1994.

Zhao, X., and J.T. Hoeksema, Effect of coronal mass ejections on the structure of the heliospheric current sheet, *J. Geophys. Res., 101*, 4825, 1996.

Zhao, X., J.T. Hoeksema, and P.H. Scherrer, Modeling boot-shaped coronal holes using SOHO-MDI magnetic measurements, in *Proceedings of the Fifth SOHO Workshop*, in press, 1997.

J. T. Gosling, Los Alamos National Laboratory, Los Alamos, NM 87544.

J. T. Hoeksema and X. Zhao, Center for Space Science and Astronomy, HEPL 213B, MC 4085, Stanford University, Palo Alto, CA 94305-4085.

J. G. Luhmann, Space Sciences Laboratory, University of California, Berkeley, CA 94720-7450.

(Received March 31, 1997; revised December 16, 1997;
accepted December 16, 1997.)